VOLUME 113, NUMBER 26
DECEMBER 18, 1991

JOURNAL OF THE AMERICAN CHEMICAL SOCIETY

Laser Photolysis Study of the Kinetics and Mechanism of Photoinitiated Peroxyoxalate Chemiluminescence

Robert E. Milofsky and John W. Birks*

Contribution from the Department of Chemistry and Biochemistry and Cooperative Institute for Research in Environmental Sciences (CIRES), Campus Box 216, University of Colorado, Boulder, Colorado 80309-0216. *Received June 24, 1991. Revised Manuscript Received August 12, 1991*

Abstract: Kinetics of photoinitiated peroxyoxalate chemiluminescence have been studied in order to further elucidate the mechanism of the reaction. Intensity versus time profiles obtained from photolysis by a single laser pulse displayed three prominent features: (1) prompt emission rising to a maximum in less than 0.3 s and decaying by a first-order process with a time constant of ≈35 s when no imidazole catalyst is present, (2) a sharp burst of light with rise and fall constants of ≈2 s when imidazole is added postphotolysis, and (3) a broad, symmetrical emission profile having nearly identical rise and fall rate constants when imidazole is added either before or after photolysis. The broad emission profile was identified as being due to photosensitized production of H_2O_2. In this case, pseudo-first-order rate constants for the rise (r) and fall (f) of the chemiluminescence intensity versus time profile were measured as a function of initial reactant concentrations and number of laser shots used to initiate the reaction. Both the rise and fall rate constants were found to be independent of the fluorophore concentration and to vary only slightly with the number of laser shots. Imidazole has a complex and nearly identical effect on the rise and fall, the dependence on imidazole concentration increasing from first to second order as the imidazole concentration increases. A finding that both the rise and fall pseudo-first-order rate constants vary linearly with oxalate ester concentration implies that two molecules of oxalate ester are involved in the reaction. These results were confirmed by additional kinetics experiments in which photochemical generation of H_2O_2 was replaced by direct addition. The kinetics of the prompt emission and of the sharp burst resulting from postphotolysis addition of imidazole is consistent with the formation in the initial photolysis reaction of the peroxydioxalate, $ArO(C{=}O)_2OO(C{=}O)_2OAr$, where Ar represents 2,4,6-trichlorophenyl. Based on kinetics results, it is proposed that the H_2O_2-initiated reaction also produces this species, which subsequently reacts to form the high-energy intermediate capable of transferring energy to the fluorophore. New high-energy intermediates derived from the peroxydioxalate are proposed. Rate constants for the rate-limiting steps of the mechanism are derived, and a computer simulation of the mechanism is found to be consistent with the experimental results.

Introduction

In an earlier study we reported that the chemiluminescence reaction of an oxalate ester such as bis(2,4,6-trichlorophenyl) oxalate (TCPO) may be initiated photochemically in the presence of oxygen and a hydrogen atom donor (HAD) such as 2-propanol (isopropyl alcohol, IPA).[1] This discovery allows the reagent hydrogen peroxide, normally used to initiate the peroxyoxalate reaction, to be eliminated and provides an unique means of studying the reaction mechanism.

Since the discovery of the peroxyoxalate chemiluminescence reaction in the early 1960s,[2-5] the identity of the intermediate(s) responsible for exciting the fluorophore has been debated.[6-9]

(1) Milofsky, R. E.; Birks, J. W. *Anal. Chem.* **1990**, *62*, 1050–1055.

(2) Chandross, E. A. *Tetrahedron. Lett.* **1963**, *12*, 761–765.
(3) Rauhut, M. M.; Bollyky, L. J.; Roberts, M. L.; Whitman, R. H.; Iannotta, A. V.; Semsel, A. M.; Clarke, R. A. *J. Am. Chem. Soc.* **1967**, *89*, 6515–6522.
(4) Bollyky, L. J.; Whitman, R. H.; Roberts, B. G.; Rauhut, M. M. *J. Am. Chem. Soc.* **1967**, *89*, 6523–6526.
(5) Rauhut, M. M. *Acc. Chem. Res.* **1969**, *2*, 80–87.
(6) Catherall, L. B.; Cundall, R. B.; Palmer, T. F. *J. Chem. Soc., Faraday Trans. 2* **1984**, *2*, 823–834.

0002-7863/91/1513-9715$02.50/0

Although never isolated despite numerous kinetics and mechanistic studies, dioxetanedione (I) has frequently been suggested to be the key intermediate.[3-5] It was proposed that dioxetanedione may

1

transfer its energy via an electron exchange with the fluorophore, as in the chemically initiated electron exchange luminescence reaction (CIEEL).[10,11] However, reported evidence for the existence of dioxetanedione[5,12] has been shown to be equivocal.[13-15] Furthermore, kinetics studies by Catherall et al. indicate that the intermediate contains one aryl group, suggesting the structures II and III.[6,7] Catherall et al. proposed structure III as the

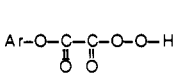

II

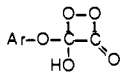

III

high-energy intermediate. Further evidence for the existence of II or III is provided by additional kinetics studies[9] and by fluorine-19 NMR of the products of the reaction of bis(2,6-difluorophenyl) oxalate with hydrogen peroxide.[16] Of course, it is possible that dioxetanedione (I) is formed from II or III by the unimolecular elimination of ArOH and is too short lived to be detected or to affect the observed kinetics.

Here we report the effects of light intensity, concentrations of imidazole, oxalate ester and chemilumophore, and the timing of catalyst addition (i.e., pre- or postphotolysis) on the kinetics of the photoinitiated chemiluminescence (PICL) reaction. In our study of the PICL reaction, we have chosen reaction conditions similar to those used by Orlovic et al.[9] in their kinetics study of the H_2O_2-initiated reaction for better comparison of the two reaction systems. The kinetics of the reaction appear to be predominantly determined by only three parameters: concentration and timing of the addition of imidazole or other nucleophile and oxalate ester concentration. The maximum and integrated chemiluminescence intensities also depend on these three parameters in addition to the excitation intensity (number of laser shots) and chemilumophore concentration. Based on the requirements for the reaction (dissolved oxygen and hydrogen atom donor), the known photochemistry of carbonyl compounds, current understanding of the H_2O_2-initiated reaction, and the observed reaction kinetics, we propose a mechanistic model for the PICL reaction.

Experimental Section

Chemicals. TCPO was purchased from Fluka Chemical Co. Rubrene, sodium methoxide, 2,4,6-trichlorophenol (TCP), and 9,10-diphenylanthracene (DPA) were obtained from Aldrich Chemical Co. KBr was obtained from Fisher, KOH, IPA, and 30% H_2O_2 from Mallinkrodt, and high-purity imidazole from Sigma Chemical Co. Ethyl acetate (spectrochemical/carbonyl free grade) was obtained from Burdick & Jackson. All chemicals and solvents were used without further purification. Stock solutions of TCPO and DPA in ethyl acetate were made at 1 and 0.5 mM concentrations, respectively, and subsequently diluted. Imidazole solutions of either 0.2 M, or 0.4 M in ethyl acetate were prepared and diluted as needed. Stock solutions of 30% hydrogen peroxide were titrated with $KMnO_4$ to determine the exact concentration of peroxide prior to dilution. Hydrogen peroxide was diluted in ethyl acetate just prior to use. All solutions were stored in the dark, and fresh solutions were prepared daily.

Chemiluminescence Measurements. In a typical experiment, 4 mL of an ethyl acetate solution of 80 mM IPA, 0.5 mM TCPO, and 0.25 mM DPA was added to a cuvette positioned in front of a PMT in a light-tight housing. The cuvette was sealed with a rubber septum, and the solution was continuously stirred by a Spectrocell stir system. All experiments were carried out at ambient temperature (298 ± 3 K).

A Lumonics Model 500 KrF excimer laser (λ = 249 nm) provided 80 mJ/pulse to the cuvette as the photolysis source. Alternatively, a low-pressure, 4.5-mW Hg lamp (λ = 254 nm) was used as the photolysis source. Timing of the laser shot (or Hg lamp) and the signal measuring electronics was accomplished using the "sync out" from the laser. Imidazole buffer (50 μL) was added by means of a Hamilton microliter syringe either immediately prior to or after photolysis to produce a final imidazole concentration of 2.5 mM (except in studies where the imidazole concentration was varied).

Luminescence was detected by photon counting, since this apparatus was already conveniently interfaced to a computer. The photocathode of a RCA 1P28 photomultiplier tube was biased at -1000 V by a Hewlett-Packard Model 6516A high-voltage power supply. The PMT was gated to receive power 300 ms after the laser fired (or the Hg lamp was extinguished) in order to eliminate the large background fluorescence from the chemilumophore. Photons were counted using an Ortec Model 454 pulse amplifier, Model 346 discriminator, and Model 9315 counter, and the signal from the pulse amplifier also was fed to a Nicolet Model 1170 signal averager. After the experiment was complete, the data were down loaded from the signal averager into a Zenith Model 2000 and/or a Macintosh SE/20 computer for analysis.

Reaction Rate Parameters. As described below, a broad, nearly symmetrical emission profile was obtained when imidazole was added to TCPO/IPA/DPA solutions prior to photolysis. In this case, the kinetics were found to fit the classic reaction scheme.

$$A \xrightarrow{r} B \xrightarrow{f} C \qquad (1)$$

where the chemiluminescence intensity is proportional to the concentration of species B and both reaction steps are first-order, irreversible reactions. The integrated rate equation gives

$$I = \frac{Mr}{r-f}(e^{-ft} - e^{-rt}) \qquad (2)$$

for the emission intensity as a function of time for this mechanism.[17] Using this simple model of the reaction kinetics, the two pseudo-first-order rate constants, r for the rise, and f for the fall, and the maximum intensity, M, were evaluated for all intensity-time profiles derived from the prephotolysis addition of imidazole, using a nonlinear least-squares analysis. Nonlinear regressions were performed by a Macintosh SE/20 computer using the software Kaleidograph. Such calculations involved a minimum of 300 data points, and all rate constants reported in this paper are results of a minimum of three independent experiments.

Results

Examples of intensity versus time profiles are given in Figure 1. Figure 1a illustrates the PICL signal in the absence of a catalyst, Figure 1b shows the effects of imidazole concentration on the emission profile for addition of imidazole catalyst prior to the laser pulse, and Figure 1c shows the effect of postphotolysis addition of imidazole. In the absence of a catalyst (Figure 1a), the emission intensity reaches a maximum in less than 0.3 s (the time the PMT is gated on) and decays exponentially with a time constant of ≈35 s. For the addition of imidazole prior to the laser pulse (Figure 1b), the prompt emission is suppressed, and a broad band emission profile similar to that reported for the H_2O_2-initiated reaction is observed.[9] The maximum intensity increases and the time to reach the maximum decreases with increasing imidazole concentration. When imidazole is added after the laser pulse (Figure 1c), in addition to the prompt emission and the broad-band emission, a sharp burst of light results with rise and fall constants also dependent on the imidazole concentration.

Emission Profile in the Absence of Imidazole. Solutions of 0.5 mM TCPO and 2.5 μM DPA were photolyzed using a single shot from the laser. The PICL reaction reached a maximum intensity within the 0.3 s prior to restoring power to the PMT and decayed

(7) Catherall, L. R.; Palmer, T. F.; Cundall, R. B. *J. Chem. Soc., Faraday Trans. 2* **1984**, *80*, 837-849.
(8) Alvarez, F. J.; Parekh, N. J.; Bogdan, M.; Matuszewski, B.; Givens, R. S.; Higuchi, T.; Schowen, R. L. *J. Am. Chem. Soc.* **1986**, *108*, 6435-6437.
(9) Orlovic, M.; Schowen, R. L.; Givens, R. S.; Alvarez, F. J.; Matuszewski, B.; Parekh, N. *J. Org. Chem.* **1989**, *54*, 3606-3610.
(10) Schuster, G. B. *Acc. Chem. Res.* **1979**, *12*, 366-372.
(11) McCapra, F.; Perring, K.; Hart, R. J.; Haan, R. A. *Tetrahedron Lett.* **1981**, *22*, 5087-5090.
(12) Cordes, H. F.; Richter, H. P.; Heller, C. A. *J. Am. Chem. Soc.* **1969**, *91*, 7209.
(13) White, E. H.; Wildes, P. D.; Wiecko, W. J.; Doshan, H.; Wei, C. C. *J. Am. Chem. Soc.* **1973**, *95*, 7050-7055.
(14) Decorpo, J. J.; Baronavski, A.; McDowell, M. V.; Saalfield, F. E. *J. Am. Chem. Soc.* **1972**, *94*, 2879.
(15) Chang, M. M.; Saji, T.; Bard, A. J. *J. Am. Chem. Soc.* **1977**, *99*, 5399-5403.
(16) Chokshi, H. P.; Barbush, M.; Carlson, R. G.; Givens, R. S.; Kuwana, T.; Schowen, R. L. *Biomed. Chrom.* **1990**, *4*, 96-99.
(17) Souchay, P.; Pannetier, P. In *Chemical Kinetics*; Elsevier Publishing: New York, 1967; pp 186-189.

Table I. Effect of IPA, TCPO, and DPA Concentrations on the Decay Constant for Photolysis in the Absence of Imidazole

[IPA], M	[TCPO], mM	[DPA], μM	10^2k_d, s^{-1}
0.082	0.5	2.5	2.84 ± 0.06
0.163	0.5	2.5	2.45 ± 0.34
0.327	0.5	2.5	2.02 ± 0.18
0.490	0.5	2.5	1.56 ± 0.22
0.654	0.5	2.5	1.31 ± 0.27
0.082	0.005	2.5	2.57 ± 0.29
0.082	0.01	2.5	2.64 ± 0.12
0.082	0.05	2.5	3.37 ± 0.18
0.082	0.25	2.5	2.62 ± 0.13
0.082	0.5	2.5	2.02 ± 0.18
0.654	0.5	0.062	1.43 ± 0.04
0.654	0.5	0.125	1.20 ± 0.22
0.654	0.5	2.5	1.33 ± 0.18

Table II. Effect of TCPO Concentration on r, f, M, and t_m

[TCPO], mM	10^2r, s^{-1}	10^2f, s^{-1}	M, au	t_m, s
0.0310	0.44 ± 0.14	0.43 ± 0.16	5.9 ± 2.8	177
0.0625	0.77 ± 0.05	0.80 ± 0.001	12.7 ± 1.1	128
0.125	1.01 ± 0.09	1.03 ± 0.09	54.0 ± 11.2	96.0
0.25	1.53 ± 0.44	1.46 ± 0.32	101 ± 12	67.0
0.5	3.21 ± 0.20	3.19 ± 0.19	163 ± 25	53.3

exponentially. A detailed analysis indicated that the prompt emission decayed by a multiexponential process composed of a relatively fast component having a time constant of ≈35 s under typical reaction conditions and at least one other much slower process. As seen in Table I, the first-order decay constant (k_d), obtained from plots of ln (intensity) versus time over the first 50 s, was found to be independent of TCPO and DPA concentrations, but decreased with increasing IPA concentration. Error bars given in Table I are standard deviations based on a minimum of three replicate measurements. We note that the two entries for conditions 0.082 M IPA, 0.5 mM TCPO, and 2.5 μM DPA differ by more than the overlap of their standard deviations (2.84 ± 0.06 versus 2.02 ± 0.18). The measurements were carried on different days using different solutions. Based on trends in the data, the later value appears to be low and may either be a statistical outlier or contain a systematic error.

Emission Profile for Addition of Imidazole Prior to Photolysis. Variation of the TCPO Concentration. In order to compare directly the kinetics of the PICL reaction with results for the H_2O_2-initiated reaction reported by Orlovic et al.,[9] the initial concentration of TCPO was varied at constant imidazole and DPA concentrations of 0.25 mM and 2.5 mM, respectively. Imidazole was added immediately prior to the laser pulse. The experimental data fit the theoretical model (eq 2) extremely well. All rate constants were determined using DPA as the chemilumophore, although it was found that the intensity versus time profile for rubrene is similar to that of DPA. The data in Table II show the effect of initial TCPO concentration on the rise, r, and fall, f, rate constants, the time to reach the maximum intensity, t_m, and the maximum intensity, M. Both the rise and fall rate constants were found to increase linearly with TCPO concentration, as seen in Figure 2, a and b. The maximum intensity increased with increasing TCPO concentration, while the time required to reach the maximum intensity decreased with increasing TCPO concentration.

Variation of Fluorophore Concentration. Variation of the concentration of DPA at constant TCPO and imidazole concentrations of 0.5 mM and 2.5 mM, respectively (for the addition of imidazole prior to the photolysis), had little or no effect on r, f, or t_m. However, as indicated in Table III, the maximum signal increased approximately linearly with DPA concentration up to 0.125 mM and then began to level off.

Variation of Imidazole Buffer Concentration. The effects of prephotolysis addition of imidazole on r, f, t_m, and M are given in Table IV and illustrated in Figure 1b for TCPO and DPA concentrations of 0.5 mM and 0.25 mM, respectively. Figure 3,

Table III. Effect of DPA Concentration on r, f, M, and t_m

[DPA], mM	10^2r, s^{-1}	10^2f, s^{-1}	M, au	t_m, s
0.0015	1.15 ± 0.05	1.06 ± 0.08	18.8 ± 1.3	50.0
0.0031	0.84 ± 0.02	0.83 ± 0.01	47.1 ± 0.4	51.3
0.0625	1.04 ± 0.28	0.89 ± 0.08	71 ± 3	52.7
0.125	0.86 ± 0.05	0.79 ± 0.10	143 ± 2	52.3
0.25	0.83 ± 0.18	0.76 ± 0.14	177 ± 43	49.3

Table IV. Effect of ImH Concentration on r, f, M, and t_m

[imidazole]	10^2r, s^{-1}	10^2f, s^{-1}	M, au	t_m, s
0.625	0.05 ± 0.01	0.06 ± 0.03		422
1.25	0.98 ± 0.09	0.97 ± 0.14	14.1 ± 0.2	98.0
2.5	4.18 ± 0.24	4.16 ± 0.25	14.9 ± 0.5	39.7
5.0	6.78 ± 0.72	6.81 ± 0.68	22.2 ± 2.1	28.0
10.0	27.1 ± 1.0	27.0 ± 0.9	86.5 ± 6.3	5.0

Table V. Effect of the Number of Laser Shots on r, f, and M

no. laser shots	10^2r, s^{-1}	10^2f, s^{-1}	M, au
1	3.50 ± 0.10	3.08 ± 0.55	3.88 ± 0.15
2	3.98 ± 0.72	3.20 ± 0.43	5.35 ± 0.85
3	4.29 ± 0.61	4.01 ± 0.51	9.32 ± 0.83
4	6.94 ± 0.29	3.63 ± 0.67	16.2 ± 1.6
5	4.71 ± 0.10	4.84 ± 0.24	20.8 ± 1.4

a and b, shows that the rise and fall rate constants both increase with increasing imidazole concentration. At higher imidazole concentrations, both the rise and fall reaction rates appear to increase in order with respect to imidazole. The maximum intensity also increases with increasing imidazole concentration, again increasing in order with respect to imidazole at higher imidazole concentrations.

Effect of Varying the Number of Laser Shots. Results of the effects of the number of laser shots used to initiate the reaction on the intensity versus time profiles for the prephotolysis addition of imidazole are given in Table V for TCPO, DPA, and imidazole concentrations of 0.5 mM, 0.25 mM, and 2.5 mM, respectively. For each experiment, the photolysis time was kept the same by varying the repetition rate of the laser. The maximum intensity increased with increasing number of laser shots. Also, the rise and fall rate constants increased slightly with increasing number of laser shots.

Emission Profile for Addition of Imidazole after Photolysis. While the addition of imidazole prior to the laser pulse generates an intensity plot very similar to that of H_2O_2-initiated chemiluminescence, the post-flash addition of the catalyst generates a sharp burst of light (time constants for rise and fall of the order of 2 s) in addition to the broad emission profile characteristic of H_2O_2-generated chemiluminescence (Figure 1c). The delayed addition of imidazole results in an exponential decline in the maximum intensity of the sharp burst. A plot of ln (maximum signal) versus time, Figure 4, gives a straight line with an inferred time constant for first-order decay of the intermediate responsible for this emission of 35 s. Within experimental error, this decay constant is identical with that for the prompt emission. Injection of a second imidazole solution following the sharp signal did not produce a second burst of light.

Hg Lamp Studies. In order to relate the kinetics of the PICL reaction to previous work involving detection in flowing systems,[1] emission profiles were obtained by initiating the reaction with a Hg lamp. The profiles thus obtained were qualitatively the same as for initiation by a laser pulse. As the photolysis time of a solution of TCPO/DPA/IPA was increased from 10 to 90 s, both the height of the initial rapid burst of light resulting from post-photolysis addition of imidazole and the height of the longer lived signal increased (Figure 5).

Effect of Other Nucleophiles. All of the nucleophiles tested (methoxide, OH^-, Br^-, and TCP) had a qualitatively similar effect on the chemiluminescence signal as imidazole. Addition of the nucleophile approximately 15 s after photolysis of a TCPO/rubrene (0.5 mM/0.25 mM) solution caused a large increase in signal, followed by a rapid decay.

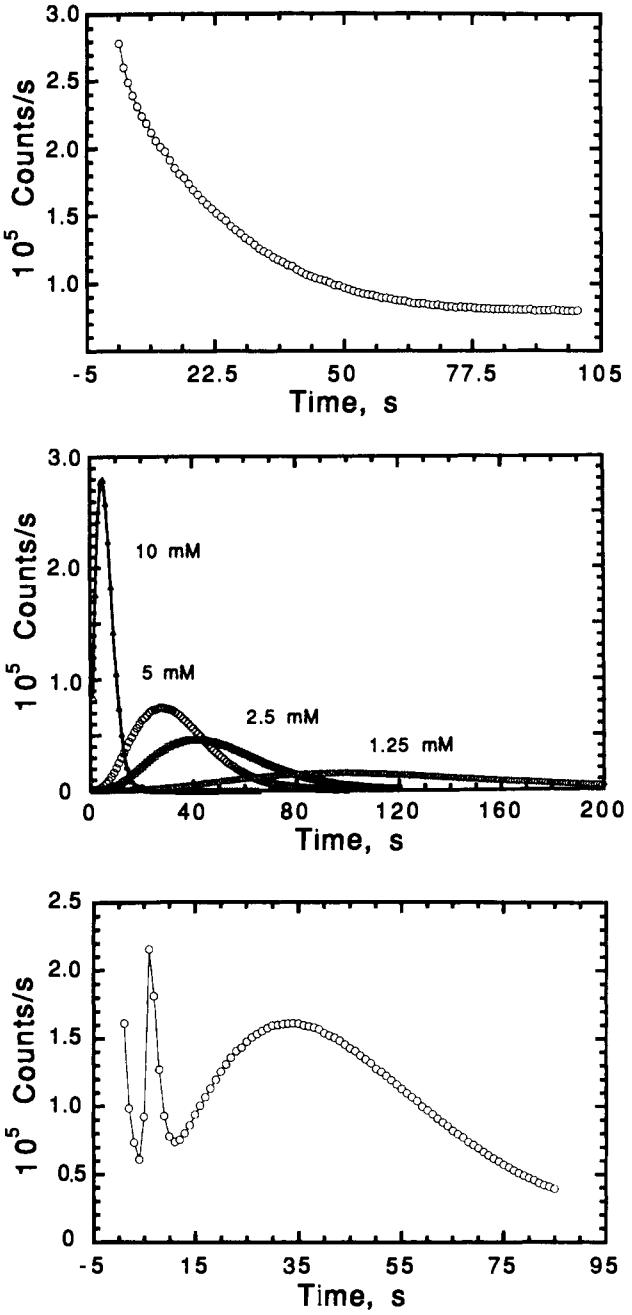

Figure 1. (a, top) Intensity vs time profile obtained in the photolysis by a single laser pulse of an ethyl acetate solution of 0.5 mM TCPO, 2.5 μM DPA, 80 mM IPA, and no imidazole. (b, middle) Intensity vs time profiles showing the effect of imidazole concentration for addition of imidazole immediately prior to the laser pulse. The high degree of symmetry of the profiles indicates that the rise and fall rate constants are nearly equal in all cases. Both the maximum intensity and the time to reach maximum intensity decrease with increasing imidazole concentration. Conditions: 0.5 mM TCPO, 0.25 mM DPA, 80 mM IPA, single laser pulse. (c, bottom) Intensity vs time profile showing the effect of addition of imidazole 10 s postphotolysis. Conditions: 0.5 mM TCPO, 2.5 μM DPA, 80 mM IPA, 1.25 mM imidazole, single laser pulse.

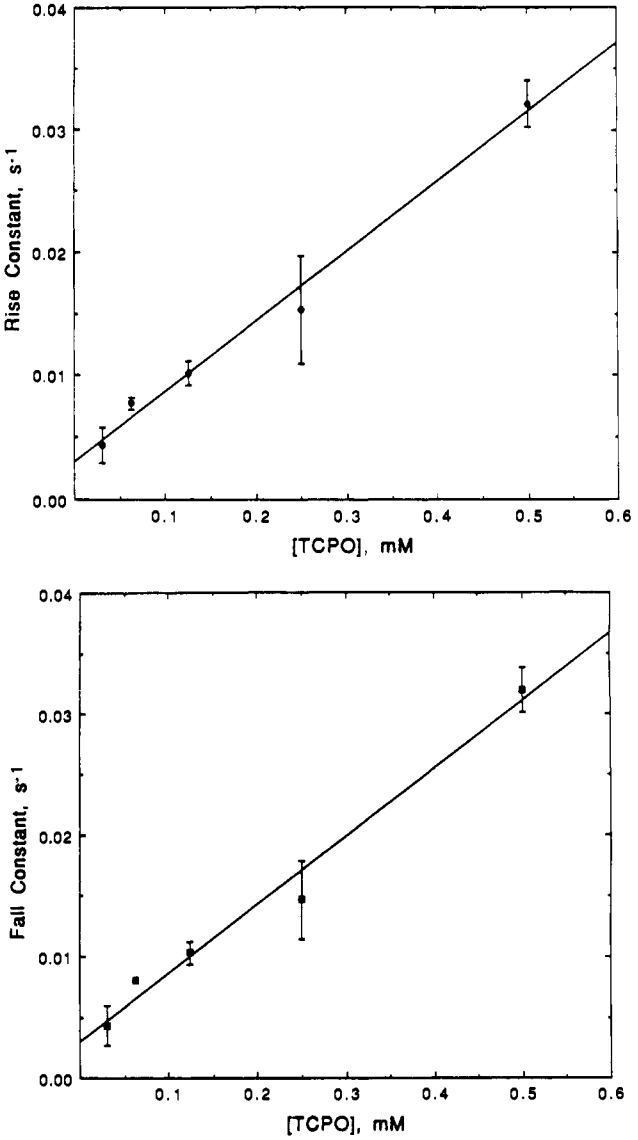

Figure 2. (a, top) Effect of TCPO concentration on the rise rate constant for the prephotolysis addition of imidazole. Conditions: 80 mM IPA, 2.5 mM imidazole, 0.25 mM DPA, single laser shot. (b, bottom) Effect of TCPO concentration on the fall rate constant for the prephotolysis addition of imidazole. Conditions: 80 mM IPA, 2.5 mM imidazole, 0.25 mM DPA, single laser shot.

Scheme I

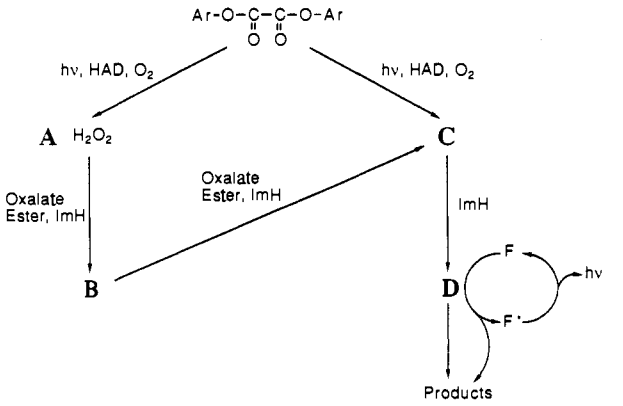

Discussion

Generalized Mechanism. The kinetics results summarized in Tables I-V, and Figure 1a-c are consistent with a mechanism, Scheme I, in which photolysis of mixtures of an oxalate ester such as TCPO, a hydrogen atom donor such as IPA, and dissolved O_2 results in the rapid formation of H_2O_2, identified as intermediate A, and another intermediate, C. The formation of C by a sequence of rapid reactions initiated by the laser pulse and its subsequent reaction with a time constant of ≃35 s to form a high-energy intermediate D accounts for the prompt emission (Figure 1a). The prompt emission is only observed in the absence of imidazole, suggesting that a precursor to the formation of C is destroyed by imidazole.

Species C is rapidly converted to the light-generating intermediate D by reaction with a variety of nucleophiles, including

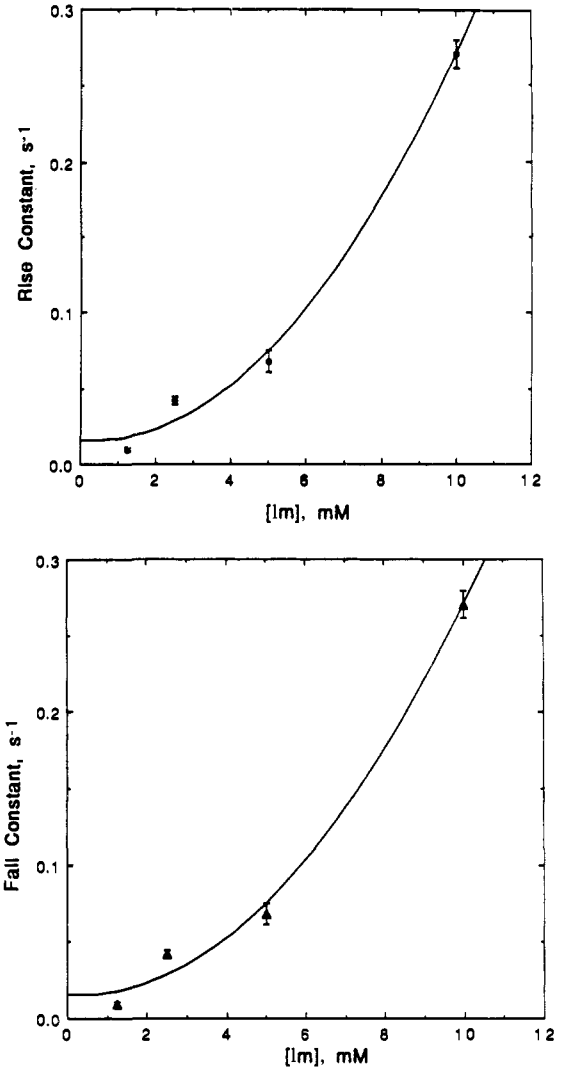

Figure 3. (a, top) Effect of imidazole concentration on the rise rate constant for the prephotolysis addition of imidazole. Conditions: 80 mM IPA, 0.5 mM TCPO, 0.25 mM DPA, single laser shot. (b, bottom) Effect of imidazole concentration on the fall rate constant for the prephotolysis addition of imidazole. Conditions: 80 mM IPA, 0.5 mM TCPO, 0.25 mM DPA, single laser shot.

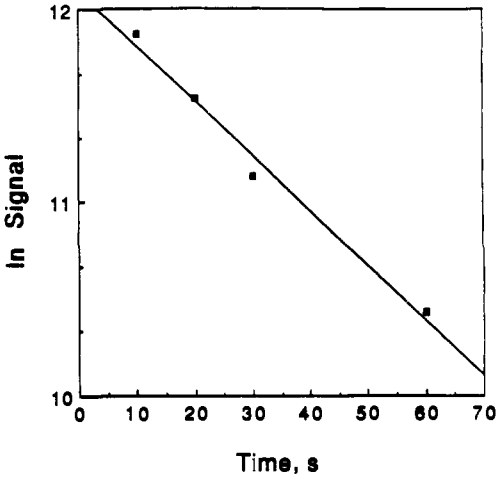

Figure 4. Plot of ln (maximum signal) of the initial burst of light as a function of the delay time between photolysis and addition of imidazole. Conditions: 80 mM IPA, 0.5 mM TCPO, 2.5 μM DPA, 1.25 mM imidazole, single laser shot.

imidazole, hydroxide ion, bromide ion, and 2,4,6-trichlorophenol, and this accounts for the sharp burst of light observed upon

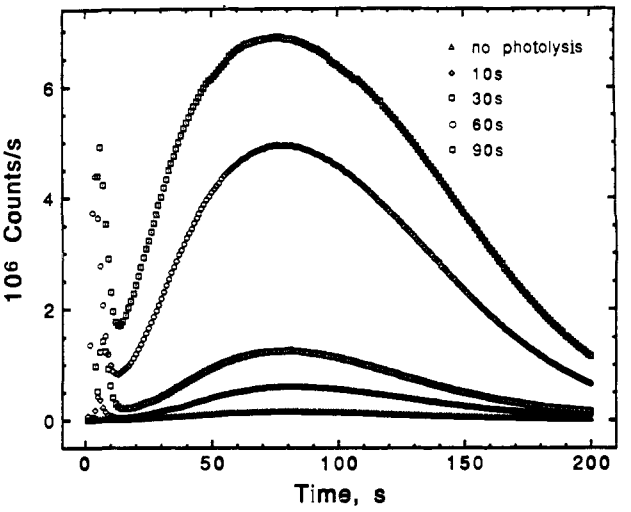

Figure 5. Effect of photolysis time by a Hg lamp on the emission profile for addition of imidazole 5 s postphotolysis. Conditions: 80 mM IPA, 0.5 mM TCPO, 2.5 μM DPA, 2.5 mM imidazole.

postphotolysis addition of any of these species. That the maximum intensity of the sharp burst for delayed addition of imidazole decays with a time constant identical with that describing the prompt emission is evidence that intermediate C is the source of both of these emissions. The sharp burst is observed only for the postphotolysis addition of imidazole, again suggesting that imidazole destroys an intermediate necessary to the formation of C.

The reaction of hydrogen peroxide with the oxalate ester to form intermediate B is catalyzed by imidazole. Kinetics results indicate that the principal loss of B is also an imidazole-catalyzed reaction with TCPO. For reasons given below, we assign C to be the product of this reaction as well. Again, in the presence of nucleophiles, C is rapidly converted to the light-generating intermediate D.

Kinetics of the H_2O_2-Generated Signal. It is likely that absorption of light by TCPO sensitizes the formation of hydrogen peroxide according to the following mechanism:

$$\text{TCPO} + h\nu \rightarrow \text{TCPO}^* \quad (3)$$

$$\text{TCPO}^* + \text{RH}_2 \rightarrow \text{HTCPO}^\cdot + \text{RH}^\cdot \quad (4)$$

$$\text{HTCPO}^\cdot + \text{O}_2 \rightarrow \text{HO}_2^\cdot + \text{TCPO} \quad (5)$$

$$\text{RH}^\cdot + \text{O}_2 \rightarrow \text{HO}_2^\cdot + \text{R} \quad (6)$$

$$\text{HO}_2^\cdot + \text{HO}_2^\cdot \rightarrow \text{H}_2\text{O}_2 + \text{O}_2 \quad (7)$$

where RH_2 is the hydrogen-atom donor (i.e., IPA). An upper limit to the concentration of hydrogen peroxide formed by this mechanism may be calculated from the integrated laser intensity ($I = 1.0 \times 10^{17}$ photons cm^{-2}), area of cuvette irradiated (A = 2 cm^2), extinction coefficient of TCPO at 249 nm (ϵ = 1000 L mol^{-1} cm^{-1}), path length (l = 1 cm), concentration of TCPO ($c = 5.0 \times 10^{-4}$ mol L^{-1}), volume of solution ($V = 4 \times 10^{-3}$ L), an upper limit to the quantum yield (Φ = 1), and Avogadro's number (N_A) using the expression:

$$[\text{H}_2\text{O}_2] = \frac{IA\Phi}{N_A V}(1 - 10^{-\epsilon lc}) \quad (8)$$

For these conditions, an upper limit to the concentration of H_2O_2 formed is calculated to be 5.7×10^{-5} M. Based on peak intensities in experiments described below, the actual concentration of H_2O_2 produced in a single laser pulse was estimated to be 1×10^{-5} M or about 50 times less than $[TCPO]_0$.

Kinetics of the broad emission band, identified as H_2O_2-initiated chemiluminescence (Figure 1b), was studied in detail in order to confirm its assignment. Rate constants for the reaction of photogenerated H_2O_2 with TCPO were derived from the intensity versus time profiles and are included in Table VI. Both the rise

Table VI. Reactions and Rate Constants Associated with H_2O_2-Initiated Chemiluminescence

reaction	rate constant[a]
H_2O_2 + TCPO → B	6.0
H_2O_2 + ImH + TCPO → B	6.0×10^3
H_2O_2 + 2ImH + TCPO → B	4.8×10^6
B + TCPO → C	6.0
B + ImH + TCPO → C	6.2×10^3
B + 2ImH + TCPO → C	4.6×10^6
C → D	2.9×10^{-2}
C + ImH → D	2×10^2
D + F → F* + products	fast
F* → F + $h\nu$	fast

[a] Units are s^{-1} for first-order reactions, $M^{-1}\ s^{-1}$ for second-order reactions, $M^{-2}\ s^{-1}$ for third-order reactions, and $M^{-3}\ s^{-1}$ for fourth-order reactions.

and fall rate constants associated with the broad emission band in PICL were found to exhibit a complex dependence on the imidazole concentration. The dependence of the rise rate constant on imidazole concentration can be described as increasing from first order to second order as the concentration of imidazole is increased. An explanation is suggested by the work of Kirsch and Jencks.[18,19] These investigators report other imidazole-catalyzed reactions of esters whose rate laws contain terms that are both first and second order in imidazole and propose that imidazole may catalyze itself by a process known as "base catalysis of imidazole catalysis by imidazole itself." The first-order dependence arises from either general base or nucleophilic catalysis, and the second-order dependence arises from a combination of both. This explanation was first applied to the imidazole concentration dependence of H_2O_2-initiated peroxyoxalate chemiluminescence in buffered acetonitrile/water solutions by Orlovic et al.[9] They observed a combination of first- and second-order dependence on the fall constant but only a first-order dependence on the rise constant. However, in their kinetics experiments, H_2O_2 was always in large excess over TCPO. In our nonaqueous system, imidazole, which is an amphoteric species, also strongly affects the acid–base chemistry, and this may contribute to the complex dependence of the rise and fall constants on the imidazole concentration.

The rise constant increases linearly with TCPO concentration (Figure 2a) as expected, confirming that the reaction is pseudo-first-order in H_2O_2 with [TCPO] ≫ [H_2O_2]. A second-order polynomial fit to the plot of rise rate constant versus imidazole concentration (Figure 3a),

$$r = a + b[\mathrm{ImH}] + c[\mathrm{ImH}]^2 \qquad (9)$$

yields the rate constants $k_1 = a/[\mathrm{TCPO}]$ for the conversion of TCPO to intermediate B in the absence of imidazole, $k_2 = b/[\mathrm{TCPO}]$ for the reaction first order in imidazole, and $k_3 = c/[\mathrm{TCPO}]$ for the reaction second order in imidazole.

Imidazole has an almost identical effect on the fall constant (Figure 3b) as on the rise constant, and the rate of destruction of intermediate B is first order in TCPO (Figure 2b). The transition from a first-order to second-order dependence on imidazole and the first-order dependence on TCPO concentration can again be explained by imidazole catalysis of the reaction of intermediate B with TCPO. A similar fit of the polynomial

$$f = d + e[\mathrm{ImH}] + f[\mathrm{ImH}]^2 \qquad (10)$$

to the plot of fall rate constant versus imidazole concentration, Figure 3b, gives values of $k_4 = d/[\mathrm{TCPO}]$ for the loss of B by reaction with TCPO in the absence of imidazole, $k_5 = e/[\mathrm{TCPO}]$ for the loss of B due to a reaction first order in imidazole, and $k_6 = f/[\mathrm{TCPO}]$ for the loss of B in the reaction second order in imidazole.

A striking result evident in Table VI is that imidazole and TCPO have nearly identical effects on the formation of B as on the destruction of B. Within experimental error, $a = d$, $b = e$, $c = f$, and the slopes of a and b in Figure 2 (effects of TCPO concentration on the rise and fall constants) are identical. Qualitatively, this can be inferred from the high degree of symmetry of the emission profiles (Figure 1b). We have concluded that this result is fortuitous. Even though the rise and fall rates are determined by reaction with the same chemical species, the rise and fall rate constants need not be identical. The same complex functional dependence on imidazole concentration by the rise and fall constants, however, implies that the two reactions share a common step, i.e., imidazole base catalysis of the nucleophilic reaction of imidazole with TCPO.

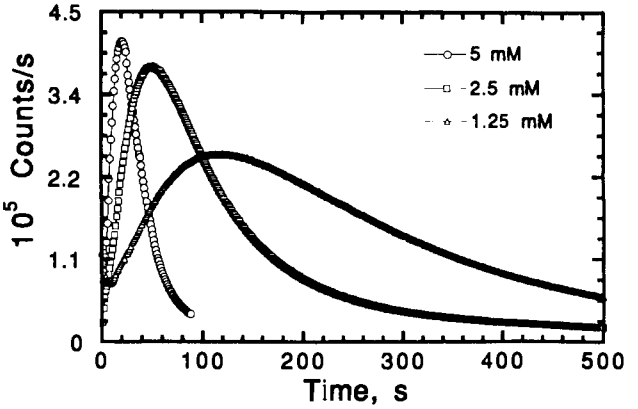

Figure 6. Effect of imidazole concentration on the emission profiles for H_2O_2-initiated chemiluminescence. Conditions: 0.5 mM TCPO, 0.25 mM DPA, 5.0 μM H_2O_2.

Figure 6 shows the intensity versus time profiles for solutions of TCPO (0.5 mM) and DPA (2.5 μM) spiked to 5 μM in H_2O_2 without photolysis, while varying the concentration of imidazole from 1.25 to 5 mM. At very low H_2O_2 concentrations (pseudo-first-order with $[\mathrm{TCPO}]_0/[\mathrm{H_2O_2}]_0 = 100$), the emission profile for the H_2O_2-initiated chemiluminescence in the presence of imidazole is nearly symmetric, and the rise and fall constants vary in the same way with imidazole concentration as does the broad-band region of the PICL emission profile. It is evident, for example, from Figures 1b and 6 that the emission maxima occur at the same times for particular imidazole concentrations in both PICL and in H_2O_2-initiated chemiluminescence. Furthermore, the rise and fall constants again vary linearly with TCPO concentration when H_2O_2 is added directly to the reaction mixture rather than being generated photochemically. From the virtually identical nature of the kinetics we conclude that the broad-band portion of the PICL signal is the result of photosensitized formation of H_2O_2. It should be noted, however, that neither the prompt emission nor the sharp burst obtained upon delayed addition of imidazole occurs in reactions initiated by direct addition of H_2O_2.

The number of laser shots used to initiate the reaction primarily affects the concentration of H_2O_2 formed, and hence the increase in maximum intensity with increasing number of laser shots. Under pseudo-first-order conditions with $[\mathrm{TCPO}]_0 \gg [\mathrm{H_2O_2}]$, the rate constants should not vary with H_2O_2 concentration. However, both the rise and fall constants appear to increase slightly with increasing number of laser shots (Table V). This could be the result of small changes in the acid-base chemistry as the extent of photolysis increases; e.g., the concentration of 2,4,6-trichlorophenol (TCP) and its anion increases as the number of laser shots increases.

Proposed Specific Mechanism In earlier work[1] we found that PICL and H_2O_2-initiated chemiluminescence exhibit the same qualitative features, including (1) catalysis by imidazole, (2) greatly enhanced response to amino-substituted polycyclic aromatic hydrocarbons (amino-PAH) as compared to the corresponding unsubstituted compounds, (3) the same general trend in sensitivity (varying over two orders of magnitude) toward individual amino-PAH compounds, and (4) a linear response to chemilumophore concentration. These similarities suggest that the two methods of initiation produce the same high-energy intermediate(s). However, the steps leading up to these intermediates are necessarily different. A proposed specific mechanism beginning with

(18) Kirsch, J. F.; Jencks, W. P. *J. Am. Chem. Soc.* **1964**, *86*, 833–836.
(19) Kirsch, J. F.; Jencks, W. P. *J. Am. Chem. Soc.* **1964**, *86*, 837–846.

Scheme II

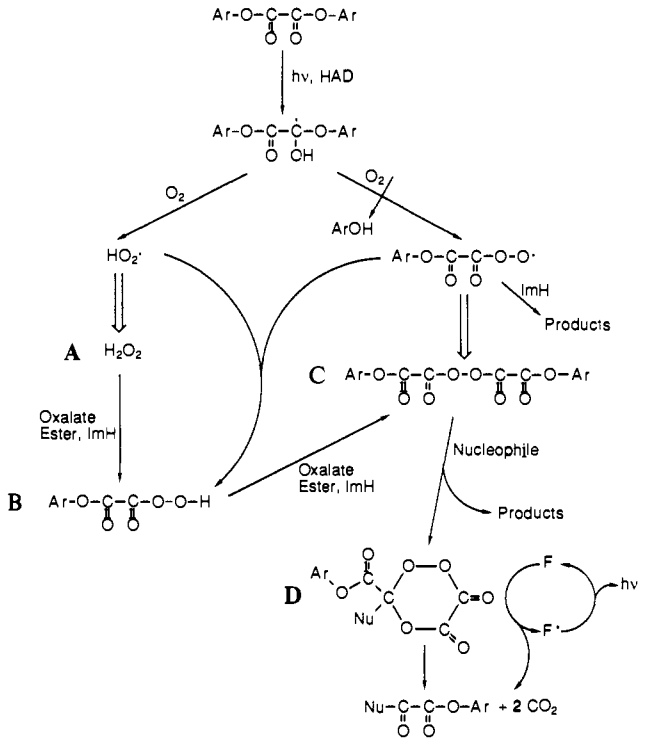

the photolysis of an oxalate ester is given in Scheme II.

It is useful to note that the production of any of the proposed high-energy intermediates, I–II, from TCPO is a reductive oxygenation; i.e., it requires the addition of two electrons (or hydrogen atoms) and two oxygen atoms. In the classical reaction, this is accomplished by reaction of TCPO with H_2O_2. The peroxyoxalate reaction may also be electrochemically initiated[20] by reduction of TCPO in the presence of O_2 or by the addition of a strong reducing agent such as $NaBH_4$ or Zn particles, again in the presence of O_2.[1] As previously described,[1] the photoinitiated reaction requires the presence of both dissolved O_2 and a hydrogen-atom donor such as isopropyl alcohol (a very weak reducing agent). Based on the well-known photochemistry of carbonyl compounds,[21] it is highly likely that the PICL reaction is initiated by the one-electron reduction of triplet-excited TCPO by the hydrogen-atom donor,

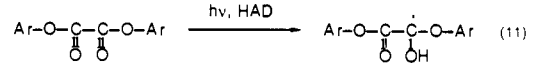

Two possible fates of the radical thus formed include reaction with O_2 to form the HO_2 radical and regenerate TCPO,

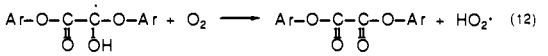

and addition of oxygen and elimination of phenol to form a peroxy radical:

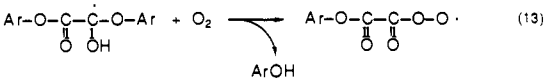

As discussed earlier, the HO_2 radical will undergo a disproportionation reaction to generate H_2O_2 (reaction 7), and as in earlier mechanisms proposed for peroxyoxalate chemiluminescence, species B is expected to be formed by the imidazole-catalyzed nucleophilic reaction of H_2O_2 with the oxalate ester:

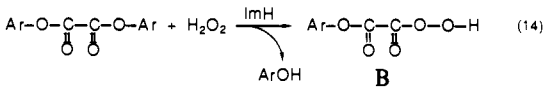

In the absence of strong reducing agents, RO_2 radicals are known to disproportionate to form organic peroxides:[22]

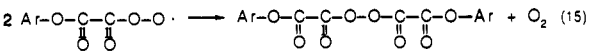

C

The peroxydioxalate product would be expected to be a marginally stable compound and to have a lifetime in solution of seconds to minutes. We propose that it is species C of Scheme I. Finally, the HO_2 radical and the peroxy radical may react to form the peroxy acid intermediate B of Scheme I:

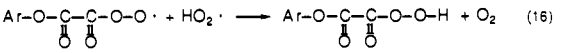

The direct formation of intermediate B in the photolysis reaction can explain the slow component of the multiexponential decay of the prompt emission.

The observation that B decays with a first-order dependence on TCPO concentration and with the same complex dependence on imidazole concentration implies that B undergoes a nucleophilic reaction with TCPO analogous to H_2O_2. The expected product (analogous to reaction 14) is the peroxydioxalate, species C:

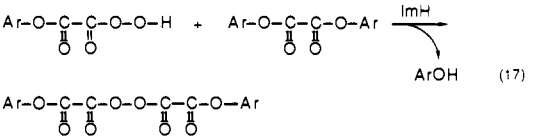

Since the reaction of C with imidazole to form D and other products is fast (≈2 s) compared to the reaction of B to form C, the B → C reaction is rate limiting and the chemiluminescence intensity for the broad band emission is proportional to the concentration of B, as required by the fit to eq 2 for the A → B → C sequence of successive reactions.

In our proposed mechanism, the peroxydioxalate C is common to the prompt emission, the sharp burst, and the broad-band emission. In the absence of addition of imidazole of other nucleophiles, it decays by a reaction having a first-order decay constant of approximately 35 s to form the light-generating species D. The sharp burst of light occurs upon addition of imidazole or other nucleophile post photolysis to accelerate the reaction. The decay in the absence of added nucleophiles may be due to reactions with TCP and/or H_2O_2 produced in the photolysis reaction.

Nucleophilic attack could occur at either one of the two inner or two outer carbonyls of C. Attack at either of the outer carbonyls would result in displacement of the good leaving group ArOH. However, attack at either of the inner carbonyls could result in nucleophilic addition followed by intramolecular nucleophilic displacement to form a cyclic peroxide, which we hypothesize to be the high-energy intermediate, D.

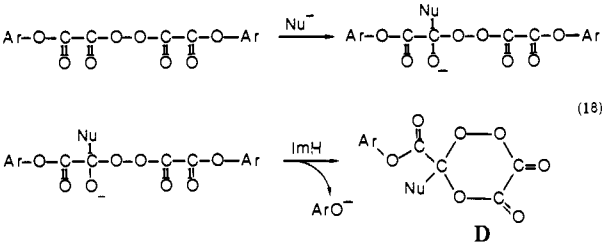

A rise constant for the sharp burst of approximately 2 s for an imidazole concentration of 2.5 mM requires a second-order rate constant for this reaction of only 200 L mol^{-1} s^{-1}. Thus, with a small rate constant, this reaction can occur on a short time scale compared to reactions 14 and 17 because of its intramolecular nature; i.e., the order of the reaction is lower. Any displacement of TCP by nucleophilic attack by imidazole at either of the outer carbonyls would only act to catalyze reaction 18. Imidazole attack at an inner carbonyl could also displace the peroxy acid species B. The effect on the kinetics would be only to reduce the effective

(20) Brina, R.; Bard, A. J. *J. Electroanal. Chem.* **1987**, *238*, 277–295.
(21) Turro, N. J. *Photochemistry of Carbonyls*; Benjamin: New York, 1981; pp 362–392.
(22) Kochi, J. K. *Free Radicals*; Wiley: New York, 1973; pp 59–60.

(measured) rate constant for reaction 17. Furthermore, the peroxy acid anion is not a good leaving group.

A consideration of resonance structures suggests that the inner carbonyls of the peroxydioxalate are particularly subject to nucleophilic addition, and the cyclic species D is an excellent candidate for the high-energy intermediate. We believe that a cyclic species is required for efficient energy transfer, because a noncyclic species such as C must form two radicals upon decomposition. The six-membered ring of D has no strain, while its decomposition produces two CO_2 molecules in addition to forming the carbonyl of the oxalate ester. By contrast, the strain of the four-membered rings of structures I and III suggest that their formation from II has a large activation energy and may even be endothermic.

Mann and Grayeski[23] have shown that emission spectra in the absence of a fluorophore for reactions of different oxalate esters with H_2O_2 have a common feature near 450 nm, attributed to phosphorescence of CO_2, and a feature at longer wavelengths with spectral shape dependent on the oxalate ester employed. The latter is attributed to emission by a decomposition product of a high-energy intermediate that contains an aromatic group derived from the ester used. Thermal decomposition of species D would be expected to produce triplet states of both CO_2 and the nucleophile-substituted oxalate ester. A possible test of our hypothesized intermediate D is to determine whether the emission spectrum in the absence of a fluorophore varies upon addition of different nucleophiles to the reaction mixture. Such an experiment would need to be carried out under conditions of low H_2O_2 concentration relative to the oxalate ester.

The lifetime of D must be less than or equal to that of C, which is 35 s in the absence of imidazole and of the order of 2 s in the presence of 2.5 mM imidazole. This explains the difficulty in identifying the high-energy intermediate of peroxyoxalate chemiluminescence; a short lifetime implies a low steady-state concentration. Experiments such as the fluorine-19 NMR studies of Chokshi et al.[16] aimed at determining the structure of an intermediate having the same kinetic behavior as the chemiluminescent emission are likely to identify intermediate B, not D, because of its much higher concentration.

A slowing of the kinetics of H_2O_2-initiated chemiluminescence by IPA added to aqueous solution was reported by Weinberger[24] and attributed to steric effects within the solvent cage. This could also account for the effect of IPA concentration on the prompt emission observed here.

The independence of the kinetics on the chemilumophore concentration is also observed in the H_2O_2 reaction[8,9] and is explained if the rates that destroy D are much faster than its chemiexcitation of the chemilumophore. The alternative, that every molecule of D is effective at transferring its energy to the fluorophore, as suggested by Orlovic et al.,[9] is ruled out by the fact that intensity increases linearly with fluorophore concentration over many orders of magnitude.[1] The observed deviation from linearity at high DPA concentration can be explained either by increased competition of the chemiexcitation step with the other loss processes or by an inner filter effect in the optically thick solution.

Finally, we would like to point out other interesting possibilities for high-energy intermediates derived from the peroxydioxalate C under the more common conditions of high concentration of H_2O_2. Nucleophilic attack of H_2O_2 at the outer carbonyl of C could produce an eight-membered cyclic intermediate, E.

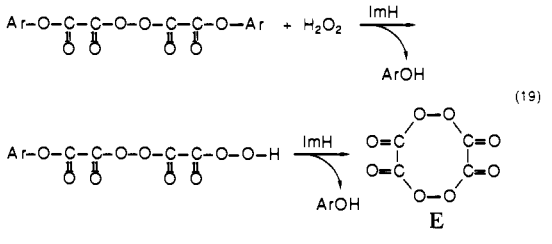

This cyclic peroxide has the advantage of being formed with no ring strain, but could eliminate up to four CO_2 molecules in the process of exciting the fluorophore. This intermediate might be especially important when H_2O_2 is in high concentration.

The peroxydioxalate C is thermodynamically unstable with respect to decomposition to carbon dioxide and acyl radicals. Furthermore, photolysis of oxalate esters could produce acyl radicals directly. These radicals could add oxygen and disproportionate with elimination of O_2 as follows:

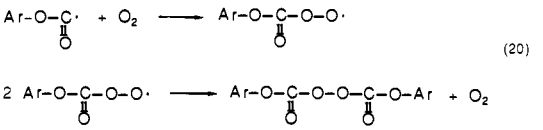

Nucleophilic reaction of the acyl peroxide with H_2O_2 could produce a six-membered cyclic peroxide F.

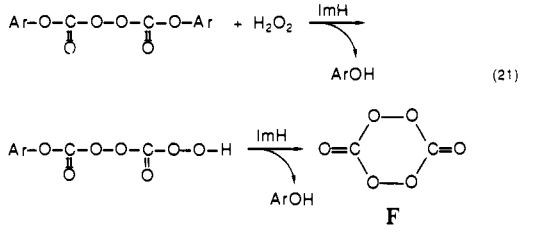

The six-membered peroxide F would be expected to form more readily than the eight-membered peroxide E. Its decomposition would release the energy associated with forming one O_2 and two CO_2 molecules. Of course, both E and F would be more likely to form when H_2O_2 is in high concentration, unlike the reaction conditions of the experiments described here.

For nearly equal concentrations of oxalate ester and H_2O_2, Alvarez et al.[8] reported two maxima in the emission profiles of the H_2O_2-initiated peroxyoxalate reaction in ethyl acetate, whose relative intensities depended on the concentration of triethylamine catalyst used. They showed that the mechanism requires the formation of two intermediates, labeled X and Y, and a third intermediate, Z, that intervenes between them. The intermediates X and Y are not themselves capable of generating light, but are postulated to react in rate-limiting steps to form two different high-energy intermediates, X′ and Y′. This is required in order for the emission profile to exhibit two maxima. Our peroxydioxalate intermediate C could be Z of their mechanism, with two of the species D, E, and F as the light-generating intermediates. As hydrogen peroxide concentration and catalyst concentration are changed, the relative rates of formation of D, E, and F would be expected to change.

The mechanism of Scheme II is speculative, especially considering that the postulated intermediates have not yet been isolated and positively identified. However, if progress is to be made in understanding the peroxyoxalate reaction, it is important to hypothesize structures for the intermediates that make good chemical sense. An important hypothesis proceeding from this work is the proposed role of the peroxydioxalate C in both PICL and H_2O_2-initiated chemiluminescence. Mass spectrometry of photolyzed solutions of TCPO in ethyl acetate, using flow injection analysis with a thermospray interface and positive fast atom bombardment (FAB) ionization, gave no evidence for C. However, this species is expected to be thermally unstable and probably decomposed in the source region of the mass spectrometer. Further efforts to isolate and identify this and other intermediates are in progress. Despite the uncertainties that remain, photoinitiation of the peroxyoxalate chemiluminescence reaction has allowed us to probe the reaction kinetics and mechanism in a way that has provided new insights.

The mechanism given in Scheme II, along with the rate constants given in Table VI and estimated from other data presented here, was input to a numerical kinetics model using the software Gear[25] and a Zenith Model 2000 computer. All of the qualitative

(23) Mann, B.; Grayeski, M. L. *Anal. Chem.* **1990**, *62*, 1536–1542.
(24) Weinberger, R. *J. Chromatogr.* **1984**, *314*, 155–165.
(25) Stabler, R. N.; Chesick, J. *Int. J. Kinet.* **1978**, 461–469.

features observed experimentally could be reproduced by the model, and plots had t_m, maximum intensities, and shapes that corresponded well with the experimental plots. This excellent correlation between the computer model and the data provides support for the kinetics representation summarized in Schemes I and II, but it is possible that other kinetics schemes could fit the data equally well.

The model has been extremely useful in optimizing concentrations and flow rates for obtaining the maximum chemiluminescence signal in analytical applications. For example, we have been able to optimize the conditions in HPLC detection of chemilumophores such as PAH and amino-PAH, as well as dansyl hydrazone derivatives of carbonyl compounds[26] so as to "capture" the signal at its maximum as the reaction products move through the detection cell. This maximum was found to correspond to the sharp burst observed in postphotolysis addition of imidazole. In this way PICL detection limits in flow injection analysis have been improved by a factor of 2 since our earlier paper.[1]

Acknowledgment. We thank Tad Koch, Gary Molander, and Richard Givens for helpful discussions of this work.

Registry No. TCPO, 1165-91-9; IPA, 67-63-0; DPA, 1499-10-1; peroxyoxalate, 119666-18-1; imidazole, 288-32-4.

(26) Nondek, L.; Milofsky, R. E.; Birks, J. W. *Chromatographia* **1991**, *32*, 33–39.

Heats of Formation of Oxygen-Containing Organic Free Radicals from Appearance Energy Measurements

John L. Holmes,* F. P. Lossing, and Paul M. Mayer

Contribution from the Chemistry Department, University of Ottawa, Ottawa, Ontario, Canada K1N 6N5. *Received April 24, 1991*

Abstract: The appearance energy method for investigating free radical thermochemistry has been shown to produce reliable heats of formation and bond strengths of organic free radicals. The present work centers on the heats of formation at 298 K of hydroxy-substituted alkyl radicals, which, for the most part, are unknown. The present results, in general, agreed well with the limited data available from the literature and are given an uncertainty of ±3 kcal mol^{-1}. It was found that hydroxy substitution in the methyl, ethyl, 1- and 2-propyl, and 2-methylpropyl radicals reduces both primary and secondary C–H bond strengths. The degree of reduction depends on the position of the substituent relative to the bond broken and is greatest for a primary bond with an α-hydroxy group, ~10 kcal mol^{-1}. The result for the hydroperoxy radical, $\Delta H_f°(HO_2\cdot) = 3.5$ kcal mol^{-1}, is in excellent agreement with the literature data, whereas the value obtained for the *tert*-butylperoxy radical, $\Delta H_f°((CH_3)_3COO\cdot) = -25.2$ kcal mol^{-1}, differs significantly from the literature value. Radical heats of formation were also measured for $\cdot CH_2CH_2OH$ ($\Delta H_f° = -13.5$ kcal mol^{-1}), $CH_3\dot{C}HOH$ ($\Delta H_f° = -14.5$ kcal mol^{-1}), $\cdot CH_2CH_2CH_2OH$ ($\Delta H_f° = -16.0$ kcal mol^{-1}), $\cdot CH_2CH(OH)CH_3$ ($\Delta H_f° = -23.0$ kcal mol^{-1}), $\cdot CH_2C(OH)(CH_3)_2$ ($\Delta H_f° = -35.2$ kcal mol^{-1}), $CH_3\dot{C}HCH_2OH$ ($\Delta H_f° = -18.8$ kcal mol^{-1}), $(CH_3)_2\dot{C}OH$ ($\Delta H_f° = -25.6$ kcal mol^{-1}), $HOCHCH_2OH$ ($\Delta H_f° = -52.6$ kcal mol^{-1}), $\cdot CH_2C(O)OH$ ($\Delta H_f° = -61.6$ kcal mol^{-1}), $\cdot CH_2C(O)OCH_3$ ($\Delta H_f° = -57.5$ kcal mol^{-1}), $\cdot CH_2OCH_2CH_3$ ($\Delta H_f° = -10.6$ kcal mol^{-1}), $\cdot C(O)OH$ ($\Delta H_f° = -46.0$ kcal mol^{-1}), $\cdot C(O)OCH_3$ ($\Delta H_f° = -39.9$ kcal mol^{-1}), $HC(O)O\cdot$ ($\Delta H_f° = -37.7$ kcal mol^{-1}), $CH_3C(O)O\cdot$ ($\Delta H_f° = -51.7$ kcal mol^{-1}).

Introduction

Recent work from this laboratory[1,2] has clearly demonstrated that the use of electron impact induced dissociative ionization of selected molecules can lead to accurate values for the heat of formation of organic free radicals. The criteria necessary for the success of such experiments have been described in detail.[2] In general, the work to date[1-4] has mostly centered upon free radicals for which results had been obtained by conventional kinetic studies of gas-phase reactions[5] or equilibrium data measured by electron paramagnetic resonance spectroscopy.[6] However, inspection of the last detailed collection[7] of $\Delta H_f°$ values for free radicals and related bond strengths shows a considerable lack of reliable data for oxygen-containing free radicals, and so the present work was undertaken.

Experimental Section

The apparatus used and its operation has been described.[8] Fragment ion–radical pairs were generated in the gas phase by impact of an energy-resolved electron beam from an electrostatic electron monochromator. The appearance energy (AE) of a given ion was determined by detecting the threshold for an ion current at the appropriate mass as the energy of the electron beam was increased in 0.02-eV steps. The energy scale was calibrated against H_2O. The apparatus and sample inlet systems operated at room temperature.

Normal and metastable ion (MI) mass spectra were recorded using a VG ZAB-2F mass spectrometer.[9]

Compounds were of the highest purity commercially obtainable.

Results and Discussion

Table I contains the results obtained for the radicals studied. All $\Delta H_f°$ values used hereafter are for 298 K. Parent molecules with heats of formation obtained from Benson additivity[10] have an estimated uncertainty in their heats of formation of ±1 kcal mol^{-1}. The error for those molecules listed in Pedley et. al.[11] is

(1) Holmes, J. L.; Lossing, F. P.; Maccoll, A. *J. Am. Chem. Soc.* **1988**, *110*, 7339.
(2) Holmes, J. L.; Lossing, F. P. *J. Am. Chem. Soc.* **1988**, *110*, 7343.
(3) Holmes, J. L.; Lossing, F. P. *Int. J. Mass Spectrom. Ion Phys.* **1984**, *58*, 1133.
(4) Holmes, J. L.; Lossing, F. P. Terlouw, J. K. *J. Am. Chem. Soc.* **1986**, *108*, 1086.
(5) Tschuikow-Roux, E.; Salomon, D. R. *J. Phys. Chem.* **1987**, *91*, 699. Tschuikow-Roux, E.; Salomon, D. R.; Paddison, S. *J. Phys. Chem.* **1987**, *91*, 3037. Tschuikow-Roux, E.; Paddison, S. *Int. J. Chem. Kinet.* **1987**, *19*, 15.
(6) Castelhano, A. L.; Griller, D. *J. Am. Chem. Soc.* **1982**, *104*, 3655.
(7) McMillen, D. F.; Golden, D. M. *Annu. Rev. Phys. Chem.* **1982**, *33*, 493.
(8) Lossing, F. P.; Traeger, J. C. *Int. J. Mass Spectrom. Ion Phys.* **1976**, *9*, 19.
(9) Burgers, P. C.; Holmes, J. L.; Szulejko, J. E.; Mommers, A. A.; Terlouw, J. K. *Org. Mass Spectrom.* **1983**, *18*, 254.
(10) Benson, S. W. *Thermochemical Kinetics*, 2nd ed.; Wiley-Interscience: New York, 1976.
(11) Pedley, J. B.; Naylor, R. D.; Kirby, S. P. *Thermochemical Data of Organic Compounds*, 2nd ed.; Chapman and Hall: New York, 1986.

0002-7863/91/1513-9723$02.50/0